SNAKES ON A PLANE:
A PERFECT SNAP FOR BIOIMAGE ANALYSIS

Ricard Delgado-Gonzalo, Virginie Uhlmann, Daniel Schmitter, and Michael Unser

In recent years, there has been an increasing interest in getting a proper quantitative understanding of cellular and molecular processes [1, 2]. One of the major challenges of current biomedical research is to characterize not only the spatial organization of these complex systems, but also their spatio-temporal relationships [3, 4]. Microscopy has matured to the point that it enables sensitive time-lapse imaging of cells *in vivo* and even of single molecules [5, 6]. Making microscopy more quantitative brings important scientific benefits in the form of improved performance and reproducibility. This has been fostered by the development of technological achievements such as high-throughput microscopy. A direct consequence is that the size and complexity of image data are increasing. Time-lapse experiments commonly generate hundreds to thousands of images, each containing hundreds of objects to be analyzed [7]. These data often cannot be analyzed manually because the manpower required would be too extensive, which calls for automated methods for the analysis of biomedical images. Such computerized extraction of quantitative information out of the rapidly expanding amount of acquired data remains a major challenge. The development of the related algorithms is non trivial and is one of the most active fronts in the new field of bioimage informatics [8, 9, 10, 11]. Segmenting thousands of individual biological objects and tracking them over time is remarkably difficult. A typical algorithm will need to be tuned to the imaging modality and will have to cope with the fact that cells can be tightly packed and may appear in various configurations, making them difficult to segregate.

In this paper, we review one of the most popular segmentation methods: 2D active contours (a.k.a. snakes). We present an extended and inclusive taxonomy of different variants of snakes for bioimage analysis. We also lay out general design principles that can help one to create new parametric snakes adjusted to different imaging modalities.

In the following section, we provide the historical context in which active contours have been developed. Then, we review the major challenges that drive the development of new snakes in the field of bioimage informatics. The next sections serve as a tutorial to design parametric snakes, representations, and energies. Finally, we give an overview of related open-source tools and packages that implement such methods while tackling real biomedical challenges.

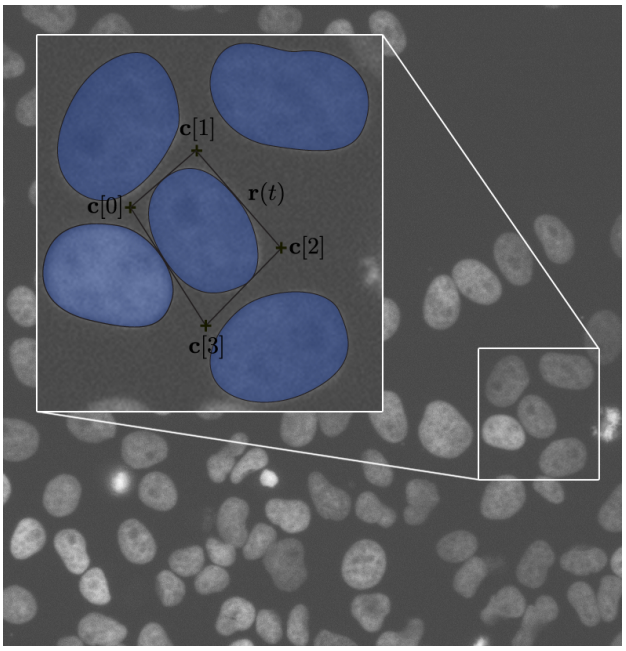

Fig. 1: Representation of the capabilities of parametric active contours at outlining HeLa nuclei in a fluorescence microscopic image. On the central cell, two contours are depicted: the parametric contour and the control polygon. The parametric contour $\mathbf{r}(t)$ is shown as a solid line enclosing a shaded region and corresponds to the actual segmentation result. The '+' elements represent the location of the free parameters of the model $\mathbf{c}[k]$. The latter define the control polygon through which the user interacts: this polygon can be adjusted to change the shape of the enclosed parametric curve.

SNAKES IN A NUTSHELL

Deformable models have gained popularity in segmentation and tracking applications [12] since they provide an excellent tradeoff between flexibility and efficiency. Within this category, active contours, also called snakes, are very popular tools for image segmentation. It can indeed be observed that among the roughly 12,000 publications about active contours indexed by Thomson Reuters' "Web of Knowledge", about 2,000 have appeared within the past three years.

In essence, an active contour is a curve that evolves within an image from some initial position towards the boundary of

the object of interest, in our case, a biological target. We show in Figure 1 the authors' favorite snakes segmenting a group of HeLa nuclei within a microscopic image. The initial position of the snake is usually specified by the user, or else is provided by an auxiliary rough detection algorithm. The evolution of the snake is formulated as a minimization problem. The associated cost function is usually referred to as *snake energy*.

Snakes have become popular because they facilitate user interaction, not only when specifying initial positions, but also during the segmentation process. The user is typically provided with tools to easily control the shape of the snake. Research on active contours has been fruitful and has resulted in many variants. They usually differ in the type of representation and in the choice of the energy term. The choice and design of both the representation and energy of the snake highly depends on the application and image modality.

CURRENT CHALLENGES

In the particular case of active contours for bioimage segmentation, several issues can be identified [13, 14]. In the following we describe ongoing challenges for snake algorithms.

Robustness and stability

Active contours are intended to be practical. It is therefore of utmost importance to ensure robustness under real-life imaging conditions where sources of image degradation include noise, bias field, and low contrast. Such image artifacts often appear in biological data. Guaranteeing stability in their presence is a major challenge to ensure the usability of algorithms.

Multi-target interaction

Bioimages rarely feature only one object of interest. In most situations, several targets, as well as undesired structures such as water bubbles or dust particles, are present in the image. Hence, a major requirement for efficient segmentation is to avoid confusion between nearby targets. Active contours must be designed so as to be able to discriminate between close or even overlapping objects, which is difficult to achieve

Flexibility and shape priors

Another requirement that snake algorithms find difficult to satisfy is to balance flexibility (to accommodate a wide range of shapes) against sufficient constraints (to secure convergence of the optimization procedure). For instance, integrating prior knowledge about the shape to segment can be used efficiently to constrain the snake, but it often remains desirable to retain the capability to adapt to variations in size, orientation, and moderate deformations.

Initialization

Snakes are semi automated algorithms. The segmentation part is mostly automated through the optimization of the snake energy, but the initialization often relies on user input. Developing automated methods to conveniently initialize active contours is an area of open research.

Snake-human interaction

Despite good initialization and efficient optimization, even the best segmentation algorithm will occasionally fail to produce satisfying results. In the case of active contours, the natural abilities of snakes to accommodate user interaction will allow one to suitably modify results in a user-friendly way.

Computational efficiency

It is crucial to provide reasonably fast implementations that run on standard computers, thereby enabling biologists to use them online for the analysis of bioimages.

Cell tracking

The last major image analysis challenge is to reliably segment thousands of individual biological objects and to track them over time. This is far from trivial due to the dependence on the imaging modality and the fact that the cells can be tightly packed in the growth chamber and may appear in various configurations making them difficult to segregate.

SNAKE TAXONOMY

Several types of snakes have been proposed over the decades. They can be broadly classified in three categories: point-, geodesic, and parametric snakes. In the following, we describe the strong and weak points of each representation while putting emphasis on parametric representations, which is the main focus of the present paper.

The first category is made of *point-snakes*, which are constructed on the most elementary representation of discrete curves. They simply consist of an ordered collection of neighboring points within a grid [15]. We show in Figure 2a an example of 2D point-snake overlaid on the grid associated to a discrete image model. The discrete curve is displayed as shaded pixels and here satisfies an 8-neighbor connectivity. Due to the discrete nature of the representation, the concept of smoothness makes no sense. However, an approximate measure of smoothness can still be defined and deployed in the energy functional of the snake. The principal drawback of this representation is that it relies on many parameters, even to encode simple shapes. The robustness of the overall segmentation algorithm hence suffers and results in a high computational complexity.

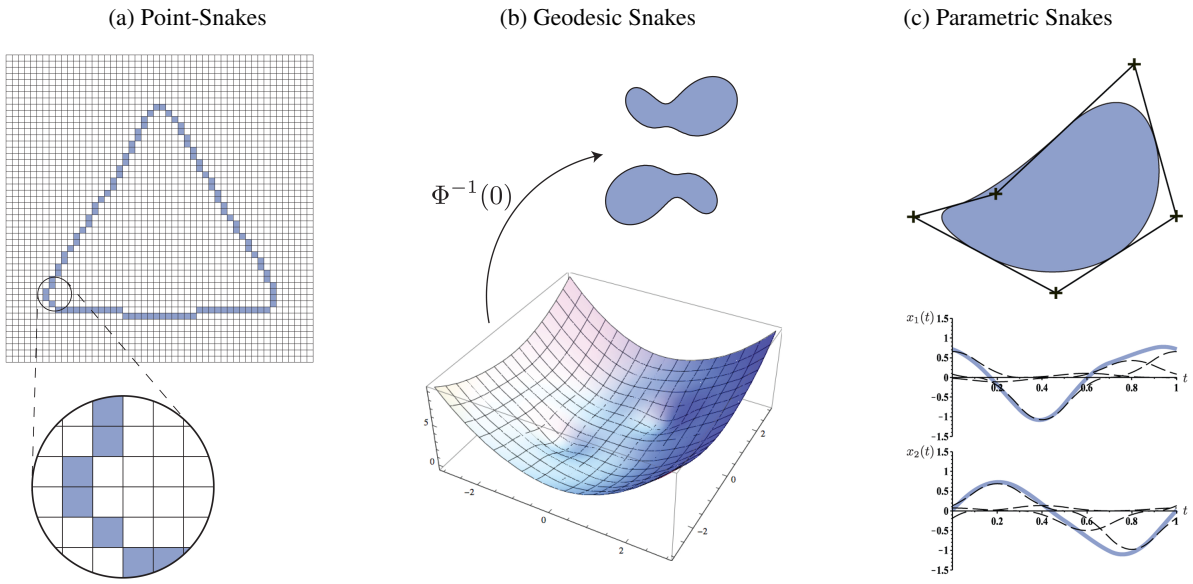

Fig. 2: Depiction of the three main families of active contours. (a) Discrete curve defined by a point-snake over the grid associated to a discrete image model. (b) Continuous curves defined as the zero level-set $\Phi^{-1}(0)$ of a scalar function Φ. (c) Continuous curve defined by a B-spline basis. The snake contour is shown as a solid line enclosing a shaded region, while the '+' elements are the control points of the spline. The parametric coordinate functions $x_1(t)$ and $x_2(t)$ are displayed in solid lines, and the dashed lines indicate the weighted basis functions.

The second category is made of *geodesic snakes*, which have been extensively used during the past decade [16, 17, 18, 19, 20, 21, 22]. These snakes are implicit, being described as the zero level-set of a higher-dimensional manifold. In the usual formalism, the snake contour is given by $\Phi^{-1}(0) = \{\mathbf{p} \in \mathbb{R}^n | \Phi(\mathbf{p}) = 0\}$, where Φ is a scalar function defined over the image domain. A unique characteristic of geodesic methods is that they can be extended to any number of dimensions. In Figure 2b, we represent a set of curves generated as the result of computing $\Phi^{-1}(0)$. This approach originates from the work of Osher and Sethian, who aimed at modeling the propagation of solid-liquid interfaces with curvature-dependent speeds [23]. In this framework, the interface (or front) is represented as a closed, nonintersecting, hypersurface flowing along its gradient field with either constant speed or a speed that depends on the curvature. Applying motion to it then amounts to solve a Hamilton-Jacob-type equation written for a function in which the interface is a particular level-set. This type of active contour has the interesting property of being particularly flexible in terms of topology. A single geodesic snake evolving under the appropriate energy functional is indeed able to split freely to segment disconnected objects within an image. This plasticity is especially convenient when segmenting complex shapes (perhaps involving significant protrusions) and when no prior assumption about the topology of the object is available. But useful geodesic models require many degrees of freedom. This makes difficult to constrain shapes and can lead to overfitting in real-world imaging conditions. Another drawback of geodesic approaches is their very expensive computational needs, mainly due to the fact that they evolve a manifold with a higher number of dimensions than the actual contour to segment. In summary, geodesic snakes, based on level-sets, are convenient when the shapes of the objects to segment exhibit high variability. However, geodesic snakes are suboptimal when segmenting known shapes.

The last category is made of *parametric snakes*. In this representation, the snake is described by some discrete set of coefficients and a continuous parameter [25, 26]. Parametric snakes are usually built in a way that ensures continuity and smoothness. Many different techniques for representing continuous curves have been published; for a review, see [27]. The continuous definition of parametric snakes suggests that the segmentation task can be conducted at arbitrary resolution, hence enabling subpixel accuracy. Another advantage is that these contours require much fewer coefficients and result in faster optimization schemes than point-snakes or geodesic snakes. In the particular case of B-spline parameterizations, the computational complexity of the energy of the snake and, therefore, the speed of the optimization algorithms, is related to the degree of overlap of the basis functions [24]. This overlap is therefore a critical parameter to consider while designing parametric snakes. User interaction is usually achieved by allowing the user to specify anchor points for the curve to go through [15]. Smoothness and shape constraints can easily be introduced [28]. They are particularly suitable when the

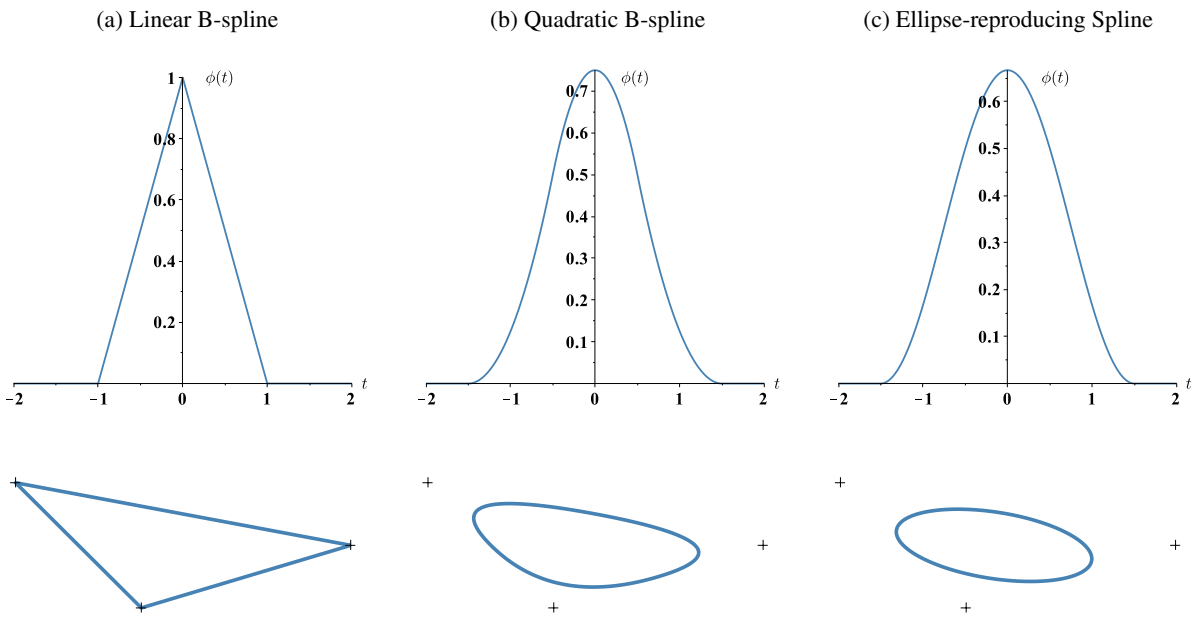

Fig. 3: Comparison between the curves generated by three different basis functions $\phi(t)$ using the same set of control points. (a) Linear B-spline, (b) Quadratic B-spline, (c) Minimum-support ellipse-reproducing spline [24].

objects to segment have a reproducible shape that can be naturally encoded within the parameterization. The most relevant example is the segmentation of circles and ellipses. In medical imaging in particular, it is desirable to segment arteries and veins within tomographic slices. Because those physiological objects are tubes, their sections show up as ellipses in the image. Ellipse-like objects are also present at microscopic scales. For instance, cell nuclei are known to be nearly circular. Similarly, water drops are spherical. However, these elements deform and become elliptical or ellipsoidal when they are subject to stress forces. For approaching these problems, ultra-fast parametric snakes were designed exploiting the properties of the parameterization, which lead to high-throughput applications [29, 30]. The downside of parametric snakes is that the topology of the curve is imposed by the parameterization. Parametric snakes are thus less suitable than geodesic ones for accommodating changes of topology during optimization, though solutions have been proposed for specific cases [31].

SPLINE-SNAKES

Curve and surface parameterizations based on Fourier descriptors [32] and uniform B-spline functions [26, 24] are popular in image processing due to the existence of efficient signal-processing algorithms and to their invariance to affine transformations. Among these, the B-spline curves have the unique advantage of featuring locality of control, hence, favoring user-friendly interactions with the snake. We show in Figure 2c an example of a curve parameterized with a B-spline basis, its spline control points, as well as its corresponding coordinate functions.

Formally, the parameterization of these snakes is expressed as a curve $\mathbf{r}(t)$ on the plane. This curve corresponds to a pair of Cartesian coordinate functions $x_1(t)$ and $x_2(t)$, where $t \in \mathbb{R}$ is a continuous parameter. The one-dimensional functions $x_1(t)$ and $x_2(t)$ are efficiently parameterized by linear combinations of suitable basis functions ϕ_k. The parametric representation of the active contour can be expressed as the vectorial equation

$$\mathbf{r}(t) = \sum_{k=0}^{M-1} \mathbf{c}[k]\, \phi_k(t), \tag{1}$$

with $\{\mathbf{c}[k]\}_{k\in\mathbb{Z}}$ a sequence of control points. The number M of control points determines the degrees of freedom in the model. Small numbers lead to constrained shapes; large numbers lead to additional flexibility and more general shapes.

In the case of spline-snakes, typical bases are those derived from a compactly-supported generator ϕ and its integer shifts $\{\phi(\cdot - k)\}_{k\in\mathbb{Z}}$. Hence, $\phi_k(t) = \phi(Mt - k)$ in (1). In this setting, fast and stable interpolation algorithms can be used [33] to compute the curve. As an illustrative example, three commonly-used functions to generate spline-snakes are represented in Figure 3. Along with the plot of the functions, the curves generated by the same set of control points and each of the depicted functions following (1) are also illustrated.

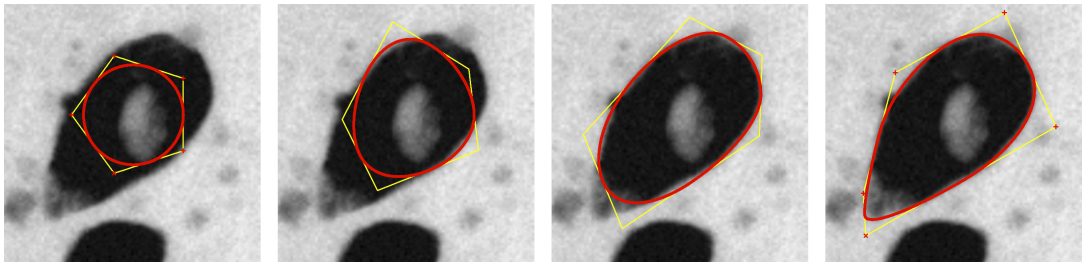

Fig. 4: Typical evolution of a parametric active contour during optimization. Left: A 5-control points snake is first initialized as a circle roughly in the center of the target cell. Center-left and center-right: Upon optimization, the contour is automatically deformed and monotonically converges from its initial position to a minimizer of the snake energy. Right: At convergence, the snake precisely outlines the target cell.

A noticeable technical feature of spline-snakes is their computational cost. Computing points on a spline curve is extremely efficient [34]. It can be shown that the expense for computing any point $\mathbf{r}(t_0)$ on the spline curve is proportional to the support of the basis function ϕ [35]. Moreover, the length of the support of a spline basis function is directly related to the degree of regularity of the function, and therefore to its approximation power [36]. Therefore, there is a trade-off between computational complexity and the approximation properties of the model. The choice of the basis function ϕ is hence influenced by two aspects: the computational complexity of the resulting segmentation algorithm, and the ability of the snake to adopt specific shapes and to retain smoothness. This has lead to research towards obtaining minimum-support basis functions that preserve good reproduction properties [24].

It is desirable for the parametric curve to satisfy several properties. Firstly, the representation should be unique and stable. The snake should indeed be defined by its coefficients in such a way that the unicity of representation of $x_1(t)$ and $x_2(t)$ is guaranteed and that the interpolation procedure is ensured to be numerically stable. This requirement translates into the so-called Riesz-basis condition on the generating function ϕ, for which space- and time-domain formulations exist. Secondly, as it is preferable for the model to be able to represent shapes irrespective of their position and orientation, invariance to affine transformations has to be enforced. This constraint yields the partition-of-unity condition, well-known in approximation theory. It implies that ϕ is capable of reproducing constants; consequently, the snake gains the ability to approximate any curve when the number of control points increases. Finally, the last common prerequisite is that the curvature of the parametric snake should be a bounded function with respect to t. This imposes for the basis ϕ, or, equivalently, for each coordinate function, to be at least $\mathcal{C}^1(\mathbb{R})$ with bounded second derivative. Starting from these three basic requirements, specific functions can be designed by imposing additional characteristics on the generator ϕ, for instance the ability to reproduce ellipses [37], or to control the tangents [38].

Under the parametric representation, snakes made of closed curves can be described with a periodic sequence of control points. In this case, both $x_1(t)$ and $x_2(t)$ are periodic with the same period. When normalized to unity such that $\mathbf{r}(t) = \mathbf{r}(t+1)$ for all $t \in \mathbb{R}$ and divided into M segments, $\mathbf{r}(t)$ involves weighted periodized basis functions. Under some mild refinability conditions, this model naturally leads to a stationary subdivision scheme. Closed parametric snakes hence appear to be particularly convenient for the segmentation of cells and cellular components.

Alternatively, open-ended active contours can also be generated with suitable basis functions. Natural conditions on the extremities of the curve typically involve two complementary interpolation functions that provide both point-wise and tangential control [38]. Such snakes have been applied to the segmentation of ridge-like objects such as chromosomes and thin rod-shaped bacteria.

ENERGY-GUIDED SEGMENTATION

The segmentation process with snakes is formulated as an energy-minimization problem. The quality of segmentation is determined by the choice of the energy terms; it is generally agreed that specific image energies need to be defined for each particular imaging device. Kass *et al.* [15] originally formulated the snake energy as a linear combination of three terms:

- the *image energy*, E_{image}, which is purely data driven;
- the *internal energy*, E_{int}, which ensures that the segmented region has smooth boundaries;
- the *constraint energy*, E_{c}, which provides a means for the user to interact with the snake.

The total energy of the snake is written as

$$E_{\text{snake}}(\Theta) = E_{\text{image}}(\Theta) + E_{\text{int}}(\Theta) + E_{\text{c}}(\Theta), \qquad (2)$$

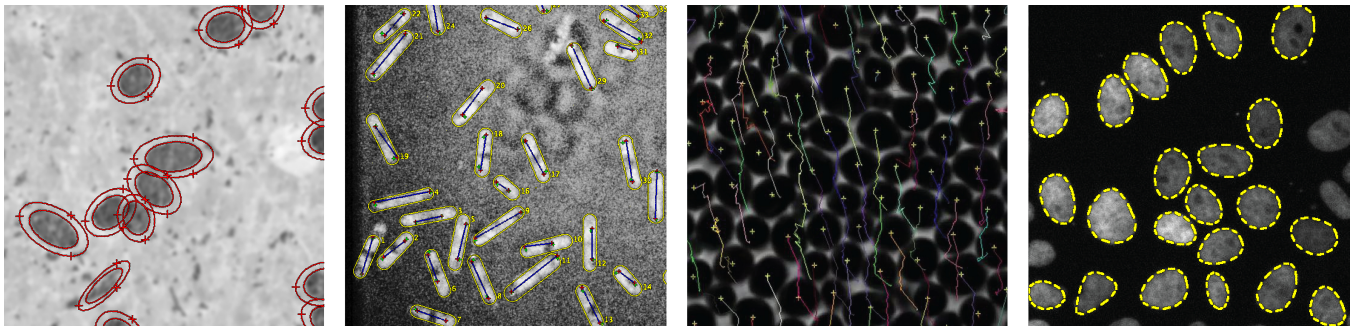

Fig. 5: Applications of parametric active contours to the segmentation and tracking. Left: Segmentation of steel needles within a cross-section of a block of concrete. The needles are cylindrical rods of identical diameter and length. Since the intersection of the plane of the cut with a cylindrical needle takes the shape of an ellipse, ovuscules are particularly appropriate tools for the task. The outer red contour represents an enclosing shell around the snake, whose volume is used to compute a region-based energy. This energy discriminates an object from its background by maximizing the contrast between the intensity of the data averaged within the volume enclosed by the snake (*i.e.*, inner contour) and the intensity of the data averaged within the volume enclosed by the shell [30]. Center-left: Segmentation of rod-shaped yeast cells of the type *Saccharomyces Cervisiae* at a large scale. The segmentation problem is coupled with the task of detecting fluorescent proteins inside the cells (red/green dots). First, the red fluorescent proteins are detected at the poles of each cell. The blue line connecting them indicates the orientation of the cell, which is used for the initialization of the snake. Because the cells all have the same shape (but different sizes), prior knowledge was integrated in the design of the snake [39]. Center-right: Segmentation and tracking of a dense set of yeast cells within phase-contrast microscopic images. In this application, the tracking was performed using a graph-based algorithm that matched snakes across time maintaining temporal consistency (*i.e.,* smooth trajectories). The snake-defining nodes were used as low-dimensionality descriptor for the inner states of the Bayesian tracker [4, 40]. Right: Segmentation of HeLa nuclei that express fluorescent core histone 2B on an RNAi live cell array [37].

where Θ encodes the snake representation (snake points, parameters, or manifolds). Then, the optimal Θ is formally obtained as

$$\Theta_{\text{opt}} = \arg\min_{\Theta} E_{\text{snake}}(\Theta).$$

The energy minimization process is nothing but an optimization procedure, where the snake representation is iteratively updated so as to reach the minimum of the energy function from a starting position. This starting position is usually specified by the user. However, many application-dependent techniques exists capable of providing a first estimate of the position of the target (*e.g.*, thresholding, DoG filtering, match filtering, watershed transform, Hough transform). In Figure 4, we illustrate the convergence of the author's favorite snake segmenting a cell. Many methods exist to minimize the energy functional (*e.g.*, gradient descent, PDEs, DP), and each optimization scheme is usually linked to a particular representation of the snake. In the case of spline-snakes, the optimization refers to iteratively updating the position of the control points, and the fastest approaches usually are gradient-based methods. These techniques require a smooth energy functional as the optimizing process relies on the computation of the partial derivative of the energy with respect to the control points, $\frac{\partial E_{\text{snake}}}{\partial \mathbf{c}[k]}$. When splines basis functions are involved, the cost of this calculation is proportional to the degree of overlap of ϕ.

The image energy is the most important of the three terms in (2) since it is the one that guides the snake to the object of interest. Traditional snakes rely on edge maps derived from the image [15, 28]. These edge-based energies can provide a good localization of the contour of the object to segment. However, they have a narrow basin of attraction, making their success depend on the quality of their initialization. Several authors have developed alternative solutions to this lack of robustness. The most important ones are the introduction of balloon forces [41], the introduction of gradient vector-fields defined everywhere on the image domain [42], or multiresolution approaches [26, 43]. Image energies can also use statistical information to distinguish different homogeneous regions [25, 30]. The region-based energies have a larger basin of attraction and can converge even if explicit edges are not present [44]. However, they provide worse localization than edge-based image energies. Image energies often require the computation of surface integrals, which are computationally expensive. Applying Green's theorem to convert them into line integrals provides a way to drastically decrease the computational load [35].

The internal energy is responsible for ensuring the smoothness of the snake. It combines the length of the contour and the curvature of the snake [15] and still corresponds to the most widely used [45]. Some authors also incorporate prior knowledge as shape constraints in this energy.

The constraint energy provides a means for the user to interact with the snake. Usually, this is obtained by introducing an energy functional that behaves as virtual springs that pull the snake towards the desired points [35]. Some implementations obviate the constraint energy while accommodating user interaction as hard constraints [37].

The parameters regulating the specifics of each energy and the tradeoff between them are usually specified by the user. In automatic pipelines, the full segmentation algorithm is trained on real images for a particular application. This usually provides a range of acceptable values that exchange robustness and acccuracy in the overall segmentation algorithm.

Instead of (2), an alternative minimization framework is the multipurpose Mumford-Shah functional. In this framework, the image is modeled as a piecewise-smooth function. The functional penalizes the distance between the model and the input image, the lack of smoothness of the model within the sub-regions, and the length of the boundaries of the sub-regions. This approach is quite popular in the context of geodesic snakes [44].

The optimization process can sometimes lead to self-intersecting snakes. This phenomenon may arise when the image energy forces some control points to move faster than others. This compromises the approach based on Greens' theorem, which assumes non self-intersecting structures and makes some snake variants unsuitable for segmenting the edges of filament-like structures (*e.g.*, axons). An extensive body of research can be found on the intersection problem, with numerous articles presenting different approaches for the intersection of freeform curves and surfaces [46]. When a self-intersection is detected, there are several ways to proceed. Some authors split their shape descriptor in a way that new smaller snakes are born [31]. Others preserve the topology by introducing self-repulsive forces [47] or opting to stop the optimization routine and ask for user assistance [37].

OPEN-SOURCE FRAMEWORK

In the context of bioimaging, an interactive and user-friendly implementation of the framework is crucial. Since parametric snakes are completely defined by their control points and the generator basis function, intuitive manipulation of the snakes can be achieved by letting the user directly move the control points with mouse-dragging gestures [29, 37]. Various ready-to-use implementations of parametric snakes are freely available as plug-ins for most popular bioimage platforms such as Fiji [10], Icy [11], and ImageJ [48]. More recently, some also have been made available for tablets. Other solutions consist in providing libraries that have active contour models integrated, such as the Insight Toolkit (ITK) that can be used to develop custom applications [49].

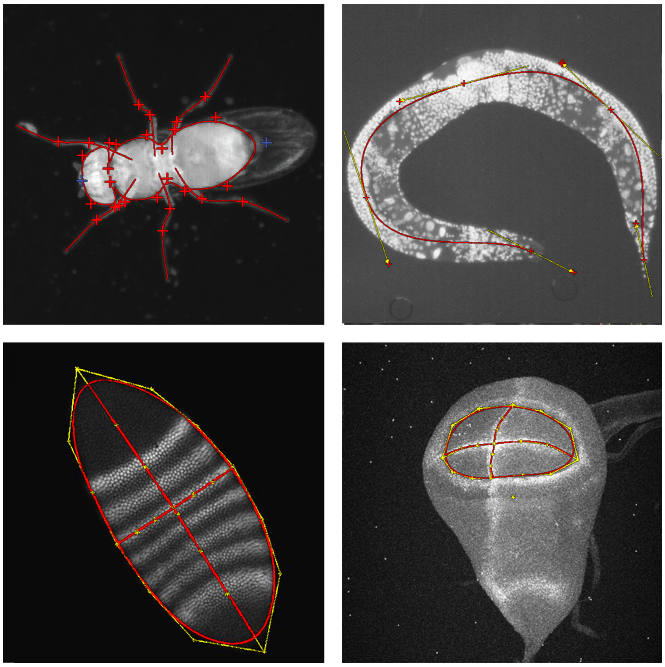

Fig. 6: Applications of parametric active contours to the segmentation of structures in organisms. The '+' elements represent the control points and their location define the effective contour of the snakes. Top-left: Segmentation of the body and legs of a *Drosophila* fly. Top-right: Detection of anteroposterior axis of a *Caenorhabditis Elegans* with nuclear staining [38]. Bottom-left: Detection of the structure of the embryo of a *Drosophila* fly within a stack of even-skipped confocal images [58]. Bottom-right: Detection of the structure of the wing pouch of a *Drosophila* fly within a stack of Wg-Ptc labeled confocal images [58].

BIOMEDICAL APPLICATIONS

The advantageous characteristics of snakes have attracted the attention of many researchers working with biological imaging data. For example, a biologist might require to segment structures at a large scale (see Figure 5), meaning that an automatic application based on high throughput analysis is required. Meanwhile, if few but large objects need to be segmented where small details are important, an interactive scheme might be more suitable (see Figure 6).

A vast literature exists on the use of snakes to segment biological structures such as biological tissues (nerve fibers [50, 51]), cell structures (mitochondria [52]), protein-based structures (actin filaments [53]), or model organisms such as zebra fish embryos [54] or *C. Elegans* (see Figure 5). The versatile nature of snakes makes them suitable for problems that combine segmentation and tracking (Leukocyte tracking [55], motility analysis [56]), organelle tracking (microtubule tracking), or even the reconstruction of cell lineages [57].

ACKNOWLEDGEMENTS

This work was funded by the Swiss SystemsX.ch initiative under Grant 2008/005 and the Swiss National Science Foundation under Grant 200020-121763 and 200020-144355.

AUTHORS

Ricard Delgado-Gonzalo (ricard.delgado@epfl.ch) was born in 1983 in Barcelona, Spain. He received two diplomas in Telecommunications Engineering and in Mathematics from the Universitat Politècnica de Catalunya (UPC) in 2006 and 2007, respectively. In 2008, he joined the Biomedical Imaging Group at the École polytechnique fédérale de Lausanne (EPFL), Switzerland, where he obtained his Ph.D. in biomedical image processing in 2013. He currently works on the design of highly efficient image-analysis open software capable of running on portable devices with an intuitive interface oriented to final users. He received the SSBE Research Award 2013 for the best Ph.D. thesis from the Swiss Society for Biomedical Engineering for his contributions to the field of bioimage informatics.

Virginie Uhlmann (virginie.uhlmann@epfl.ch) was born in Nyon, Switzerland, in 1989. From September 2011 to August 2012, she was awarded the competitive Excellence Fellowship at the Master's level from the École polytechnique fédérale de Lausanne (EPFL), Switzerland. She pursued her Master's thesis as a visiting student in the Imaging Platform, Broad Institute, Cambridge, MA, under the supervision of Anne Carpenter. She obtained her M.S. degree in Bioengineering from EPFL in September 2012 and was awarded four prizes, including third best grade point average among EPFL's M.S. graduates of 2012. She started a Ph.D. in the Biomedical Imaging Group at EPFL under the direction of Michael Unser. She is currently working on applied problem related to image segmentation and tracking, as well as on wavelet and spline theory. She is also involved in several teaching assistant duties. Her research interests also include computer vision, machine learning, and life sciences.

Daniel Schmitter (daniel.schmitter@epfl.ch) received his master diploma in Bioengineering and Biomedical Technologies from the École polytechnique fédérale de Lausanne (EPFL), Switzerland in 2013. He was with the Advanced Clinical Imaging Technology Group, Siemens, at the Center for Biomedical Imaging, Switzerland, where he was one of the main contributors working on brain-imaging software and related image-processing algorithms. Currently, he is a Ph.D. student at the Biomedical Imaging Group at EPFL, where he is working on spline-related segmentation problems. He has developed several segmentaion and tracking software in the field of biomedical imaging.

Michael Unser (michael.unser@epfl.ch) is Professor and Director of EPFL's Biomedical Imaging Group, Lausanne, Switzerland. His main research area is biomedical image processing. He has a strong interest in sampling theories, multiresolution algorithms, wavelets, the use of splines for image processing, and, more recently, stochastic processes. He has published about 250 journal papers on those topics. From 1985 to 1997, he was with the Biomedical Engineering and Instrumentation Program, National Institutes of Health, Bethesda USA, conducting research on bioimaging. Dr. Unser has held various editorial positions in the journals of the IEEE Signal Processing Society (IEEE Trans. Med. Imaging, IEEE Trans. Image Processing). He was recently elected to the board of the Proceedings of the IEEE. He co-organized the first IEEE International Symposium on Biomedical Imaging (ISBI2002) and was the founding chair of the technical committee of the IEEE-SP Society on Bio Imaging and Signal Processing (BISP). Dr. Unser is a fellow of the IEEE (1999), EURASIP fellow (2009), and a member of the Swiss Academy of Engineering Sciences. He is the recipient of several international prizes including three IEEE-SPS Best Paper Awards and two Technical Achievement Awards from the IEEE (2008 SPS and EMBS 2010).

REFERENCES

[1] Z.N. Demou, "Time-lapse analysis and microdissection of living 3D melanoma cell cultures for genomics and proteomics," *Biotechnol. Bioeng.*, vol. 101, no. 2, pp. 307–316, Oct. 2008.

[2] K. Kirkegaard, I.E. Agerholm, and H.J. Ingerslev, "Time-lapse monitoring as a tool for clinical embryo assessment," *Hum. Reprod.*, vol. 27, no. 5, pp. 1277–1285, May 2012.

[3] C. Zimmer, B. Zhang, A. Dufour, A. Thébaud, S. Berlemont, V. Meas-Yedid, and J.-C. Olivo-Marin, "On the digital trail of mobile cells," *IEEE Signal Process. Mag.*, vol. 23, no. 3, pp. 54–62, Jan. 2006.

[4] N. Dénervaud, J. Becker, R. Delgado-Gonzalo, P. Damay, A.S. Rajkumar, M. Unser, D. Shore, F. Naef, and S.J. Maerki, "A chemostat array enables the spatio-temporal analysis of the yeast proteome," *Proc. Natl. Acad. Sci. USA*, vol. 110, no. 39, pp. 15842–15847, Sept. 24, 2013.

[5] A. Miyawaki, "Visualization of the spatial and temporal dynamics of intracellular signaling," *Dev. Cell*, vol. 4, no. 3, pp. 295–305, Mar. 2003.

[6] D. Muzzey and A. Van Oudenaarden, "Quantitative time-lapse fluorescence microscopy in single cells," *Annu. Rev. Cell Dev. Bi.*, vol. 25, pp. 301–327, Nov. 2009.

[7] M. Oheim, "Advances and challenges in high-throughput microscopy for live-cell subcellular imag-

ing," *Expert Opin. Drug Disc.*, vol. 6, no. 12, pp. 1299–1315, Dec. 2011.

[8] G. Myers, "Why bioimage informatics matters," *Nat. Meth.*, vol. 6, no. 7, pp. 659–660, Jul. 2012.

[9] A. Cardona and P. Tomancak, "Current challenges in open-source bioimage informatics," *Nat. Meth.*, vol. 9, no. 7, pp. 661–665, Jul. 2012.

[10] J. Schindelin, I. Arganda-Carreras, E. Frise, V. Kaynig, M. Longair, T. Pietzsch, S. Preibisch, C. Rueden, S. Saalfeld, B. Schmid, J.-Y. Tinevez, D.J. White, V. Hartenstein, K. Eliceiri, P. Tomancak, and A. Cardona, "Fiji: An open-source platform for biological-image analysis," *Nat. Meth.*, vol. 9, no. 7, pp. 676–682, Jul. 2012.

[11] F. de Chaumont, S. Dallongeville, N. Chenouard, N. Hervé, S. Pop, T. Provoost, V. Meas-Yedid, P. Pankajakshan, T. Lecomte, Y. Le Montagner, T. Lagache, A. Dufour, and J.-C. Olivo-Marin, "Icy: An open bioimage informatics platform for extended reproducible research," *Nat. Meth.*, vol. 9, no. 7, pp. 690–696, Jul. 2012.

[12] A.P. Britto and G. Ravindran, "Review of deformable curves—A retro analysis," *Inf. Technol. J.*, vol. 6, no. 1, pp. 26–36, Jan. 2007.

[13] G. Hamarneh and X. Li, "Watershed segmentation using prior shape and appearance knowledge," *Image Vision Comput.*, vol. 27, no. 1, pp. 59–68, Jan. 2009.

[14] D. Cremers, M. Rousson, and R. Deriche, "A review of statistical approaches to level set segmentation: Integrating color, texture, motion and shape," *Int. J. Comput. Vision*, vol. 72, no. 2, pp. 195–215, Apr. 2007.

[15] M. Kass, A. Witkin, and D. Terzopoulos, "Snakes: Active contour models," *Int. J. Comput. Vision*, vol. 1, no. 4, pp. 321–331, Jan. 1987.

[16] R. Malladi, J.A. Sethian, and B.C. Vemuri, "Shape modeling with front propagation: A level set approach," *IEEE Trans. Pattern Anal. Mach. Intell.*, vol. 17, no. 2, pp. 158–175, Feb. 1995.

[17] V. Caselles, R. Kimmel, and G. Sapiro, "Geodesic active contours," *Int. J. Comput. Vision*, vol. 22, no. 1, pp. 61–79, Feb. 1997.

[18] H. Zhang, Z. Bian, Y. Guo, B. Fei, and M. Ye, "An efficient multiscale approach to level set evolution," in *Proc. 25th Annual Int. Conf. IEEE Eng. Med. Bio. Soc.*, Sept. 17-21, 2003, pp. 694–697.

[19] G. Aubert, M. Barlaud, O. Faugeras, and S. Jehan-Besson, "Image segmentation using active contours: Calculus of variations or shape gradients?," *SIAM J. Appl. Math.*, vol. 63, no. 6, pp. 2128–2154, Aug./Sept. 2003.

[20] B. Appleton and H. Talbot, "Globally optimal geodesic active contours," *J. Math. Imaging Vis.*, vol. 23, no. 1, pp. 67–86, Jul. 2005.

[21] X. Bresson, P. Vandergheynst, and J.-P. Thiran, "Multiscale active contours," *Int. J. Comput. Vision*, vol. 70, no. 3, pp. 197–211, Dec. 2006.

[22] K. Zhang, L. Zhang, H. Song, and W. Zhou, "Active contours with selective local or global segmentation: A new formulation and level set method," *Image Vision Comput.*, vol. 28, no. 4, pp. 668–676, Apr. 2010.

[23] S. Osher and J.A. Sethian, "Fronts propagating with curvature-dependent speed: Algorithms based on Hamilton-Jacobi formulations," *J. Comput. Phys.*, vol. 79, no. 1, pp. 12–49, Nov. 1988.

[24] R. Delgado-Gonzalo, P. Thévenaz, and M. Unser, "Exponential splines and minimal-support bases for curve representation," *Comput. Aided Geom. Des.*, vol. 29, no. 2, pp. 109–128, Feb. 2012.

[25] M.A.T. Figueiredo, J.M.N. Leitão, and A.K. Jain, "Unsupervised contour representation and estimation using B-splines and a minimum description length criterion," *IEEE Trans. Image Proc.*, vol. 9, no. 6, pp. 1075–1087, Jun. 2000.

[26] P. Brigger, J. Hoeg, and M. Unser, "B-spline snakes: A flexible tool for parametric contour detection," *IEEE Trans. Image Proc.*, vol. 9, no. 9, pp. 1484–1496, Sept. 2000.

[27] V.V. Kindratenko, "On using functions to describe the shape," *J. Math. Imaging Vis.*, vol. 18, no. 3, pp. 225–245, May 2003.

[28] L.H. Staib and J.S. Duncan, "Boundary finding with parametrically deformable models," *IEEE Trans. Pattern Anal. Mach. Intell.*, vol. 14, no. 11, pp. 1061–1075, Nov. 1992.

[29] P. Thévenaz and M. Unser, "Snakuscules," *IEEE Trans. Image Proc.*, vol. 17, no. 4, pp. 585–593, Apr. 2008.

[30] P. Thévenaz, R. Delgado-Gonzalo, and M. Unser, "The ovuscule," *IEEE Trans. Pattern Anal. Mach. Intell.*, vol. 33, no. 2, pp. 382–393, Feb. 2011.

[31] T. McInerney and D. Terzopoulos, "T-snakes: Topology adaptive snakes," *Medical Image Analysis*, vol. 4, no. 2, pp. 73–91, Jun. 2000.

[32] C.T. Zahn and R.Z. Roskies, "Fourier descriptors for plane closed curves," *IEEE Trans. Comput.*, vol. C-21, no. 3, pp. 269–281, Mar. 1972.

[33] M. Unser, "Sampling—50 Years after Shannon," *Proc. IEEE*, vol. 88, no. 4, pp. 569–587, Apr. 2000.

[34] M. Unser, "Splines: A perfect fit for signal and image processing," *IEEE Signal Process. Mag.*, vol. 16, no. 6, pp. 22–38, Nov. 1999.

[35] M. Jacob, T. Blu, and M. Unser, "Efficient energies and algorithms for parametric snakes," *IEEE Trans. Image Proc.*, vol. 13, no. 9, pp. 1231–1244, Sept. 2004.

[36] R. Delgado-Gonzalo and M. Unser, "Spline-based framework for interactive segmentation in biomedical imaging," *IRBM*, vol. 34, no. 3, pp. 235–243, Jun. 2013.

[37] R. Delgado-Gonzalo, P. Thévenaz, C.S. Seelamantula, and M. Unser, "Snakes with an ellipse-reproducing property," *IEEE Trans. Image Proc.*, vol. 21, no. 3, pp. 1258–1271, Mar. 2012.

[38] V. Uhlmann, R. Delgado-Gonzalo, and M. Unser, "Snakes with tangent-based control and energies for bioimage analysis," in *Proc. 11th IEEE Int. Sym. Biom. Imaging*, Apr. 29-May 2, 2014, pp. 806–809.

[39] D. Schmitter, P. Wachowicz, D. Sage, A. Chasapi, I. Xenarios, V. Simanis, and M. Unser, "A 2D/3D image analysis system to track fluorescently labeled structures in rod-shaped cells: Application to measure spindle pole asymmetry during mitosis," *Cell Div.*, vol. 8, no. 6, pp. 1–13, Apr. 27, 2013.

[40] R. Delgado-Gonzalo, *Segmentation and Tracking in High-Throughput Bioimaging*, Ph.D. thesis, EPFL, Switzerland, thesis no. 5657, 2013.

[41] L.D. Cohen, "On active contour models and balloons," *CVGIP: Imag. Understand.*, vol. 53, no. 2, pp. 211–218, Mar. 1991.

[42] C. Xu and J.L. Prince, "Snakes, shapes, and gradient vector flow," *IEEE Trans. Image Proc.*, vol. 7, no. 3, pp. 359–369, Mar. 1998.

[43] J. Tang and S.T. Acton, "Vessel boundary tracking for intravital microscopy via multiscale gradient vector flow snakes," *IEEE Trans. Biomed. Eng.*, vol. 51, no. 2, pp. 316–324, Feb. 2004.

[44] T.F. Chan and L.A. Vese, "Active contours without edges," *IEEE Trans. Image Proc.*, vol. 10, no. 2, pp. 266–277, Feb. 2001.

[45] A.K. Jain, Y. Zhong, and M.-P. Dubuisson-Jolly, "Deformable template models: A review," *Signal Process.*, vol. 71, no. 2, pp. 109–129, 1998.

[46] C.M. Hoffmann, *Geometric and Solid Modeling*, Morgan Kaufmann, first edition, 1989.

[47] C. Zimmer and J.-C. Olivo-Marin, "Coupled parametric active contours," *IEEE Trans. Pattern Anal. Mach. Intell.*, vol. 27, no. 11, pp. 1838–1842, Nov. 2005.

[48] C.A. Schneider, W.S. Rasband, and K.W. Eliceiri, "NIH Image to ImageJ: 25 years of image analysis," *Nat. Meth.*, vol. 9, no. 7, pp. 671–675, Jul. 28, 2012.

[49] L. Ibáñez, W. Schroeder, L. Ng, and J. Cates, *The ITK Software Guide*, Kitware, Inc., first edition, 2003.

[50] Y.-L. Fok, J.C.K. Chan, and R.T. Chin, "Automated analysis of nerve-cell images using active contour models," *IEEE Trans. Med. Imag.*, vol. 15, no. 3, pp. 353–368, Jun. 1996.

[51] Y. Wang, Y. Sun, C.K. Lin, and M.S. Ju, "Segmentation of nerve fibers using multi-level gradient watershed and fuzzy systems," *Artif. Intell. Med.*, vol. 54, no. 3, pp. 189–200, Mar. 2012.

[52] E.U. Mumcuoglu, R. Hassanpour, S.F. Tasel, G. Perkings, M.E. Martone, and M.N. Gurcan, "Computerized detection and segmentation of mitochondria on electron microscope images," *J. Microsc.*, vol. 246, no. 3, pp. 248–265, Jun. 2012.

[53] H. Li, T. Shen, D. Vavylonis, and X. Huang, "Actin filament segmentation using spatiotemporal active-surface and active-contour models," in *Proc. 13th Int. Conf. Med. Image Comput. Comput Assist. Interv.*, Sept. 20-24, 2010, vol. 6361, pp. 86–94.

[54] T. Wu, J. Lu, J., Y. Lu, T. Liu, and J. Yang, "Embryo zebrafish segmentation using an improved hybrid method," *J. Microsc.*, vol. 250, no. 1, pp. 68–75, Febr. 2013.

[55] N. Ray, S.T. Acton, and K. Ley, "Tracking leukocytes in vivo with shape and size constrained active contours," *IEEE Trans. Med. Imag.*, vol. 21, no. 10, pp. 1222–1235, Oct. 2002.

[56] X. Wang, H. Weijun, D. Metaxas, R. Mathew, and E. White, "Cell segmentation and tracking using texture-adaptive snakes," in *Proc. 4th IEEE Int. Sym. Biom. Imaging*, Apr. 12-16, 2007, pp. 101–104.

[57] B. Zhang, C. Zimmer, and J.-C. Olivo-Marin, "Tracking fluorescent cells with coupled geometric active contours," in *Proc. 2004 IEEE Int. Sym. Biom. Imaging*, Apr. 15-18, 2004, pp. 476–479.

[58] T. Schaffter, *From Genes to Organisms: Bioinformatics System Models and Software*, Ph.D. thesis, EPFL, Switzerland, thesis no. 6081, 2014.